A Systematic Approach Towards Integrated Safety Modelling for Aerospace Applications – Preliminary Results on Rigid Seat Simulations

Nina Wegener[1], Christoph Sauer[1], Paul Schatrow[1], Matthias Waimer[1]

[1] Institute of Structures and Design, German Aerospace Center, Stuttgart

Abstract

In the aviation sector, the historically evolved crashworthiness requirements prescribe seat certification separately from the airframe structure. Based on historical test and accident data the airframe crash behaviour is presumed in terms of crash pulses, which are applied to the seat structure for seat certification (e.g. EASA CS-23/25.562). Certification authorities have recently started to change the regulations from a prescriptive to a performance-based certification, considering the crash performance with the seats integrated in the airframe structure (EASA CS-23 Amendment 5). With this, occupant safety and structural crashworthiness is combined to an integrated safety approach. Due to the high cost of full-scale testing in the aviation sector, extensive use of simulation is of interest. Modelling methods are continuously being developed for crash loading conditions relevant to aerospace, which significantly differ from automotive ones. The German Aerospace Center (DLR) Institute of Structures and Design has extensive experience in developing simulation methods for aircraft crash analysis. In an effort to develop an integrated safety modelling approach for aviation, a research initiative was launched to incorporate advanced passenger safety considerations.

In the first phase, methodologies for modelling and simulation of current certification tests are developed. This includes seating procedures for finite element (FE) anthropomorphic test devices (ATDs) and seat belt modelling methods. Future steps include the investigation of advanced ATDs and human body models, the implementation of seat and passenger systems into structural crash models and the consideration of novel cabin layouts.

SAE Aerospace Recommended Practice 5765B defines a means of assessing the credibility of computer models of aircraft seating systems used to simulate dynamic impact conditions. This includes supplementary test data of sled tests with aerospace approved ATDs on a rigid seat, which are the basis for validation of the developed methodologies in this first phase of the project.

This paper describes a systematic approach to integrated safety modelling for aerospace applications. Additionally, preliminary results of the first phase for LSTC Hybrid 3 and Humanetics Hybrid 2 ATD models on a rigid seat are presented. The simulation study was conducted using LS-DYNA®.

1   Introduction

In the aviation sector, seats are certified separately from the airframe structure. For seat certification crash pulses are applied to the seat. The structural performance of the seat is assessed and injury criteria are evaluated from ATDs (EASA CS-(Part).562, 14 CFR (Part).562) [1-8]. The regulations exist for different aircraft categories such as small and large airplanes (Part 23 and Part 25) or small and large rotorcraft (Part 27 and Part 29), for which individual crash pulses are presumed. There are two pulses prescribed for seat certification, a pulse with 30° forward pitch, on sled tests usually executed as 60° backwards, commonly referred to as test 1, shown in Fig. 1 a) and a horizontal pulse commonly referred to as test 2 shown in Fig. 1 b). The pulse shapes are symmetrical isosceles triangles (Fig. 1 c). Each regulation, dependent on aircraft type, prescribes different acceleration magnitudes and pulse durations for the two test conditions which were derived from historical test and accident data. The regulations prescribe the use of either the Hybrid 2 or the FAA Hybrid 3 ATD. Both ATD types have a straight lumbar spine which is considered essential to measure lumbar loads for vertical impact conditions.
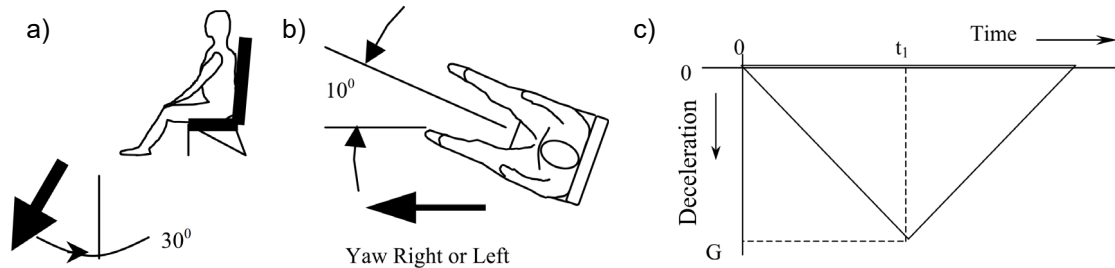
Fig.1:   Seat certification: test 1 (a), test 2 (b) and schematic pulse shape (c) [9]

In 2017 however, certification authorities have started to change the regulations from a prescriptive to a performance-based certification enabling the applicants to follow an integrated crash safety approach considering the true airframe crash performance with the seats integrated in the airframe structure (EASA CS-23 Amendment 5) [10]. However, in the aviation sector full-scale testing is very costly and there is little data available on the performance of seat systems under realistic crash conditions apart from actual incidents [11]. In this context, there is a continuous need to develop modelling methods for aerospace relevant crash loading conditions to supplement crash tests with simulations. Next to accuracy of the models used, one other important aspect of passenger safety modelling for the assessment of crash performance in early concept development is computation time of the virtual ATDs (v-ATD), especially for full-scale airplane crash simulations where a great number of v-ATDs is utilized.

2   Integrated Safety Approach: Research Plan at DLR

The DLR Institute of Structures and Design launched a research project to develop an integrated safety modelling approach for aviation to implement advanced passenger safety considerations into structural crash models, which were historically the primary focus. The aim of the project is to use a systematic approach for developing integrated crash safety concepts for airplanes, helicopters and advanced air mobility vehicles.

The first phase includes the development of the general modelling techniques used for passenger safety simulations using rigid seat tests with the LSTC FAST and LSTC DETAILED Hybrid 3 automotive v-ATDs. Part of this is the investigation of different methodologies to place the ATD model on the rigid seat. Additionally, a study of the influences of different belt materials and belt to ATD contact formulations was performed [12]. In addition to the rigid seat simulations, a drop test of a generic airplane section was simulated to include an early assessment of the applicability of the derived conclusions on realistic crash conditions. Furthermore, the developed methodologies will be applied to v-ATDs specific to aerospace applications, namely the Humanetics Hybrid 2, Hybrid 2 EXPRESS and FAA Hybrid 3 models, as well as advanced ATDs and various Human Body Models (HBM). The aim of this first phase is to establish a baseline assessment of the various models for aerospace applications as a starting point for the following phases. The second phase will focus on the modelling of realistic seat structures under sled pulse loading. The third phase will include real crash conditions and the incorporation of the realistic seats into airplane sections and full-scale models of airplanes and AAM vehicles, as well as the consideration of novel cabin layouts. This includes the integration of the models into an automated and parameterized modelling process, namely the DLR process chain PANDORA [13].

3   Methods and Models

To assess the quality of computer models for the simulation of seat certification tests, SAE Aerospace Recommended Practice 5765B [14] supplies guidelines for the modelling techniques to be used for the seat as well as evaluation criteria for v-ATD. As a basis for v-ATD validation supplementary data is provided from tests performed at NIAR. The supplied test data includes four different test configurations. Scenario 1 uses the horizontal acceleration pulse from Part 25 with a peak acceleration of 16 g, a rise time of 0.09 s and a two-point belt. This test configuration should be used mainly to evaluate head path, pelvis kinematics and belt forces. Scenario 2 uses the 60° pitch condition from Part 23 with a peak acceleration of 19 g, a rise time of 0.05 s and a two-point belt. The main purpose of this test is to evaluate the lumbar force. Scenario 3 and scenario 4 use the Part 23 horizontal pulse of 21 g peak acceleration, a rise time of 0.06 s, with a three-point and a four-point belt respectively. Scenario 3 can be used to evaluate upper chest rotation connected with the three-point belt. The focus of scenario 4 are the belt strap loads. All tests were performed on a rigid seat with fixed anchorages for the restraint system, to minimize the test variables and focus on ATD behavior. Furthermore, yaw and roll of the certification

tests were not replicated. Each test was performed with both the Hybrid 2 and the FAA Hybrid 3 ATD. The preliminary results presented in this paper will focus on scenario 1 and 2 performed with the Hybrid 2 ATD. The performance of three different virtual ATDs is assessed in comparison to the tests, the Humanetics H2 50th EXPRESS V1.0 (Fig. 2 a), the LSTC H3 50th DETAILED 190217_BETA (Fig 2 b) and the LSTC H3 50th FAST 120702_V2.0 (Fig. 2 c). The H2 EXPRESS is derived from Humanetics H2 50th V2.0, pelvis and upper legs were re-meshed to a bigger element size and all parts except pelvis, lumbar, abdomen and neck are modelled as rigid bodies to decrease run time for early development considerations. A comparison of the v-ATDs regarding number of nodes, number of elements and average runtime for the 0.2 s pulse on the rigid seat is shown in table 1. Only the Humanetics H2 EXPRESS is modelled after an aerospace approved ATD, both LSTC v-ATDs are automotive ATDs with a curved spinal column.
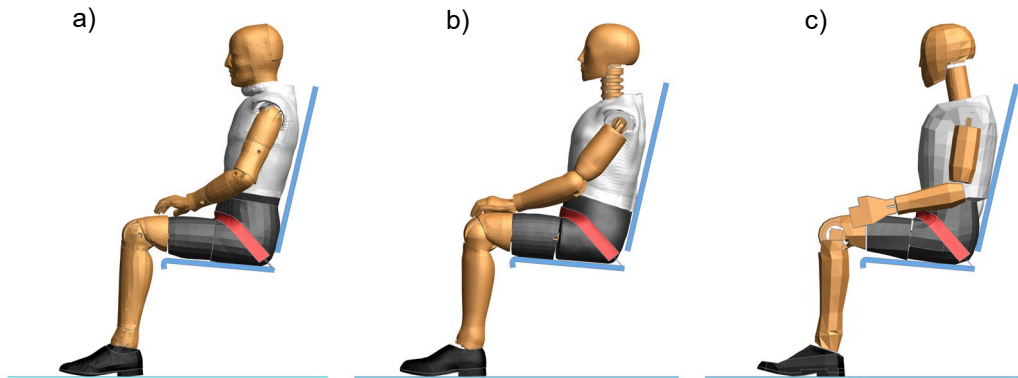
Fig.2: *V-ATDs: H2 EXPRESS (a), H3 DETAILED (b) and H3 FAST (c)*

v-ATD	No. of nodes	No. of elements	Run time
H2 50th EXPRESS V1.0	100,039	121,578	1 h
LSTC H3 50th DETAILED 190217_BETA	279,201	465,951	16 h
LSTC H3 50th FAST 120702_V2.0	7,402	4,313	0.2 h

Table 1: *V-ATD comparison*

SAE ARP 5765B allows the v-ATD to be placed into the seat by different methods, however it recommends seating using gravity loading, replicating the procedure for the physical ATD. In addition to gravity, an 89 N force is applied to the torso to push it into the seat. This procedure was used for seating for the comparison between the different v-ATD models. It should be noted that the initial position of the v-ATD is likely to vary from the physical test when using this seating method.
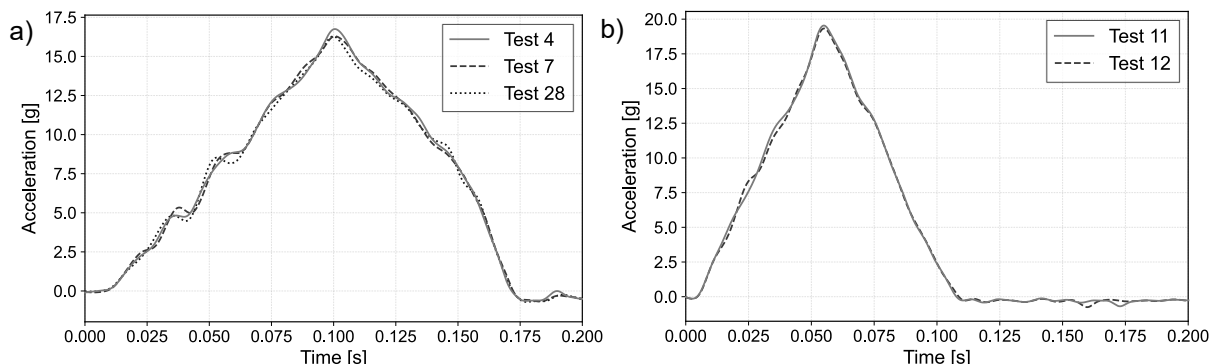

Fig.3: *Sled accelerations rigid seat tests scenario 1 (a) and scenario 2 (b).*

The sled pulses of the tests are shown in Fig. 3. For scenario 1 there are three tests, for scenario 2 there are two. SAE ARP 5765B recommends simulating each test separately for validation, using the recorded sled pulse from the test, however only one simulation per scenario is presented in this paper. For the sled accelerations of scenario 1 the recorded acceleration of test 4 is used in the simulations, for scenario 2 the acceleration data of test 11.

SAE ARP 5765B also prescribes to evaluate the correlation between test and simulation with a quantitative error metric. To evaluate the curve shape error the Sprague&Geers error is used, a separate peak error is also calculated as described in [14]. Which channels should be evaluated for the scenarios is given in the SAE ARP 5765B as well as allowable maximum error values.
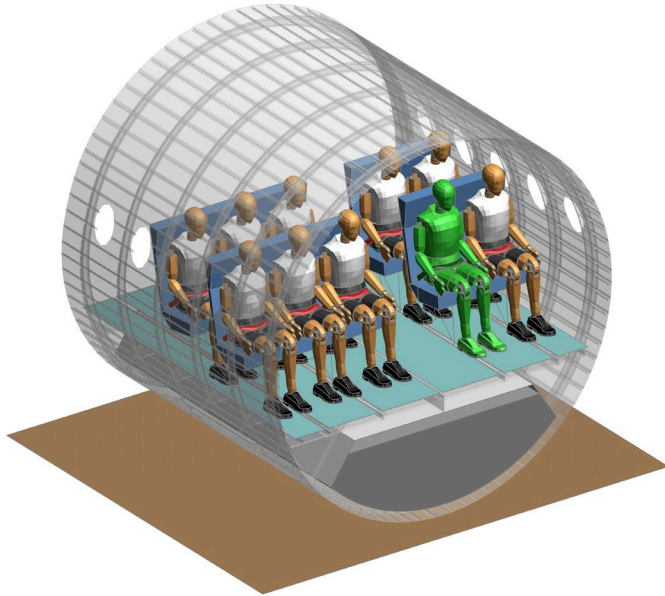

Fig.4:   Airplane section

In addition to the rigid seat tests, the v-ATDs are also evaluated simulating a drop test of a generic airplane section (Fig. 4) to investigate, if the observations made for the rigid seat simulations can be applied to more realistic crash conditions. A generic airplane section with a generic seat is used, therefore no test data is available for comparison. The airplane section is dropped on a rigid surface with an initial velocity of 7.62 m/s. The airplane section includes two rows of seats, each row with a triple and a double seat. For the comparison of the different v-ATDs only the v-ATD in the front row aisle v-ATD on the double seat was changed, highlighted green in Fig. 4. All other v-ATDs are H3 FAST models due to run time considerations.

4   Results

4.1   Rigid Seat: Scenario 1

For this scenario the H3 FAST v-ATD is not evaluated. In this model some of the internal ATD parts in the pelvis are not modelled. This leads to unrealistic deformations of the pelvis with the two-point belt and a horizontal pulse, shown in Fig. 5.
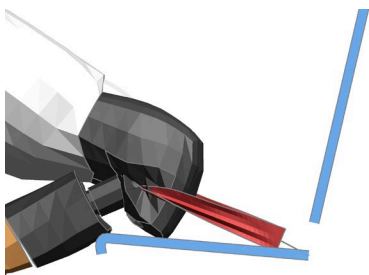

Fig.5:   Scenario 1: H3 FAST pelvis deformation

Table 2 shows the v-ATD kinematics compared to test 4. It can be observed that the H2 EXPRESS shows a slightly stiffer behavior than the H3 DETAILED, especially in the neck, which is most likely the result of the differences between the two ATD types in this region which is reflected in the respective models. The overall movement of both v-ATDs however is quite similar to the behavior observed in the tests. Although it can be seen that the pelvis of the H3 DETAILED experiences a greater deformation.

The positional data for the head center of gravity (head CG) is shown in Fig. 6 a). After 0.170 s - 0.175 s the target markers on the ATDs heads for all three tests were obscured by the legs, therefore no data could be obtained after that time. For both the H3 DETAILED and the H2 EXPRESS v-ATD the general curve shape is in good agreement with the tests. This can also be seen with the curve shape errors shown in Table 3. Here x- and z-position are evaluated separately. Both v-ATDs are well within the limit of the maximum allowable error of 10% prescribed by SAE ARP 5765B for the x-position.

Time	H2 EXPRESS	H3 DETAILED	Test 4
0 s			
0.12 s			
0.16 s			
0.2 s			
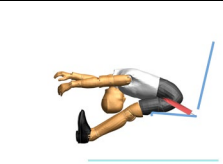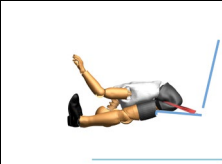
Table 2: Scenario 1: ATD kinematics

However, the H2 EXPRESS exhibits a slightly lower Z-displacement, therefore exceeding the maximum allowable curve shape error for the Z-position. Whereas the H3 DETAILED experiences a higher head excursion in X-direction, while this does not affect the curve shape error, the calculated peak error (Table 4) exceeds the allowed maximum of 12.7 mm. The peak error is between 70.20 mm, when compared to test 28, and 75.21 mm, when compared to test 7. Note that no peak error is to be calculated for the head CG Z-position.
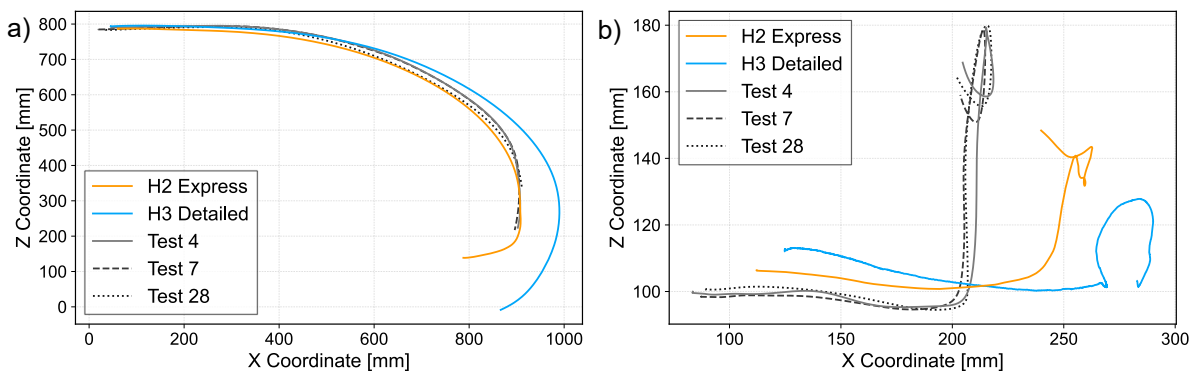

Fig.6: Scenario 1: XZ-position head CG (a) and H-Point (b)

Fig. 6 b) shows the H-Point position. Both v-ATDs start with a considerable initial offset in H-Point position compared to the tests. There are multiple possible causes for this difference in initial position. The chosen method for placing the v-ATD on the seat does not necessarily replicate the exact test position, furthermore there can be differences caused by manufacturing and wear and tear of the physical ATD which are not represented in the v-ATD [14]. For the H3 DETAILED v-ATD the difference in initial position of the H-Point is even larger, one contributing factor in this v-ATD is the differently

shaped pelvis in the automotive ATD. The X-component of the movement is comparable to the tests for both v-ATDs, most of the difference can be explained with the offset in initial position. Both v-ATDs underpredict the Z-component, which can also be seen in the calculated peak errors shown in Table 4. While the H2 EXPRESS can capture a similar behaviour for the recoil due to the seatbelt, the H3 DETAILED cannot replicate the behaviour, which could be related to the visual observation that the pelvis is deformed more in this v-ATD. Both ATDs exceed the maximum curve shape error considerably (Table 3).

		H2 EXPRESS			H3 DETAILED		
Channel	Max error	Test 4	Test 7	Test 28	Test 4	Test 7	Test 28
Head CG X Position [%]	10	3.03	6.47	4.78	2.68	5.61	4.11
Head CG Z Position [%]	10	16.34	25.28	15.32	6.10	2.33	7.32
H-Point X Position [%]	10	32.31	36.42	33.92	53.75	59.09	56.47
H-Point Z Position [%]	10	44.50	40.97	43.84	65.71	61.99	65.68
Belt Force [%]	15	11.60	12.84	11.27	17.64	18.79	17.14

Table 3: Scenario 1: curve shape error

		H2 EXPRESS			H3 DETAILED		
Channel	Max error	Test 4	Test 7	Test 28	Test 4	Test 7	Test 28
Head CG X Position [mm]	12.7	1.33	2.06	2.95	74.48	75.21	70.20
H-Point X Position [mm]	6.35	44.33	48.04	45.25	71.58	75.28	72.49
H-Point Z Position [mm]	5.08	35.91	35.18	36.45	51.50	50.78	52.05
Belt Force [%]	10	5.17	0.87	0.18	20.37	13.46	14.24

Table 4: Scenario 1: peak error

The belt force measured with the H3 DETAILED shows a good agreement in curve shape with the tests for the first 0.125 s (Fig. 7). The first local maximum can be represented well, however the global maximum is 1.2 kN higher than the highest force recorded from the tests, possibly related to the observations for H-Point position and pelvis deformation. This results in curve shape errors of 17.14 %, 17.64 % and 18.79 %, slightly exceeding the given limit of 15 % (Table 3) and peak errors of 13.46 %, 14.24 % and 20.37 % (Table 4).
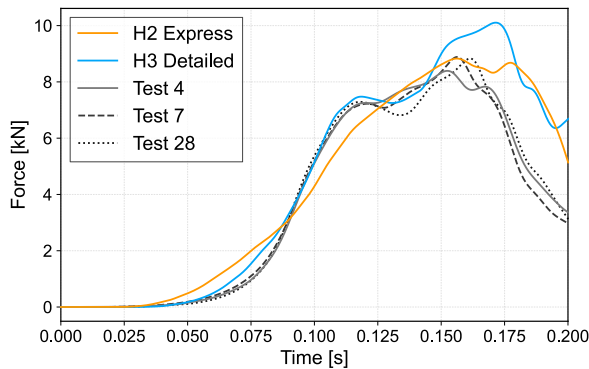

Fig.7: Scenario 1: belt force

The belt force for the H2 EXPRESS matches the tests in peak value, leading to peak errors well within the allowable maximum. It also stays within the limits for the curve shape error.
It is noteworthy that the curve shape and peak errors for the simulations are not necessarily better when compared to test 4, which is the test of which the sled pulse was used. In this case, other factors have stronger influences than the exact replication of the tested pulse.

4.2 Rigid Seat: Scenario 2

The kinematic behavior of the ATDs for scenario 2 is shown in Table 5. As seen for scenario 1, the H2 EXPRESS shows a stiffer upper body movement, which is close to the behavior observed for test 11. Both H3 v-ATDs exhibit a greater forward and downward movement of the upper body and head. This is even more pronounced in the H3 FAST.
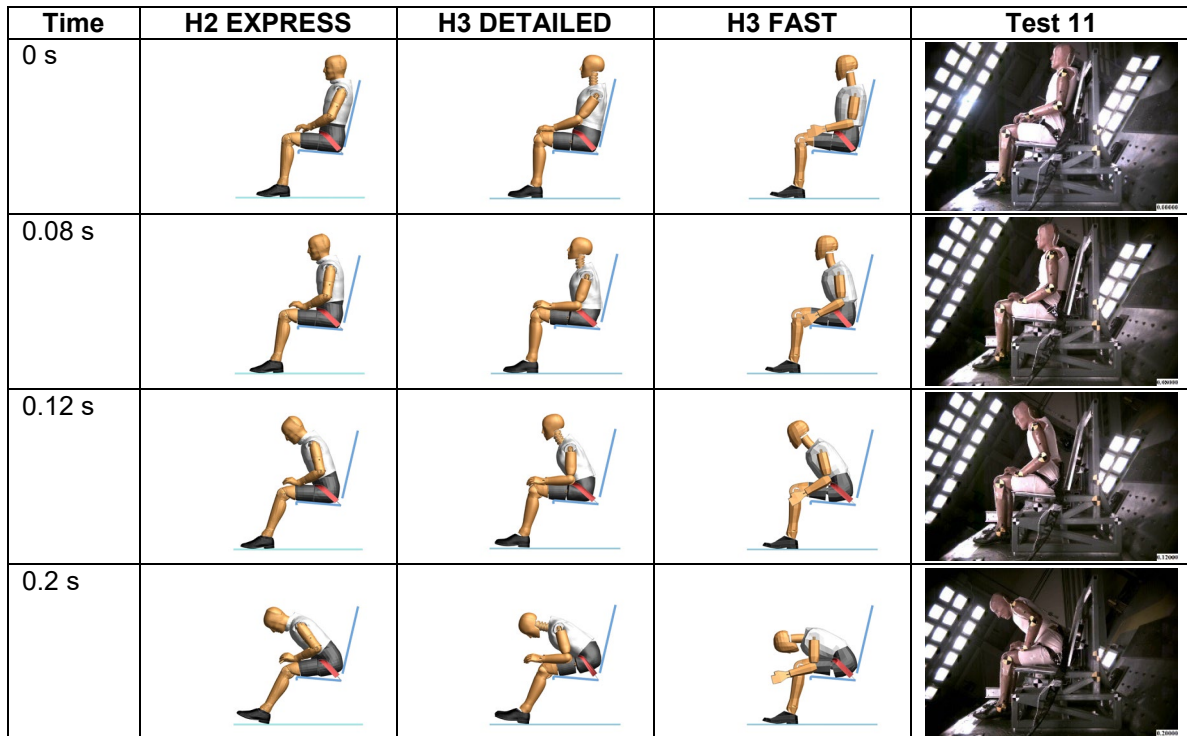
Time	H2 EXPRESS	H3 DETAILED	H3 FAST	Test 11
0 s				
0.08 s				
0.12 s				
0.2 s				

Table 5: Scenario 2: ATD kinematics

The comparison of the lumbar loads in Fig. 8 shows that all three models underpredict the maximum lumbar compression. The H2 EXPRESS exhibits the highest lumbar load with -6.5 kN. The extremum occurs 0.02 s before the tests. The H3 FAST has a peak of -4.9 kN, which is closest in timing to the tests. The H3 DETAILED has the lowest lumbar load with -4.6 kN. For both H3 v-ATDs this discrepancy is to be expected due to their curved spinal column. None of the v-ATDs achieve a curve shape or peak error within the limits specified, as seen in Table 6 and Table 7.
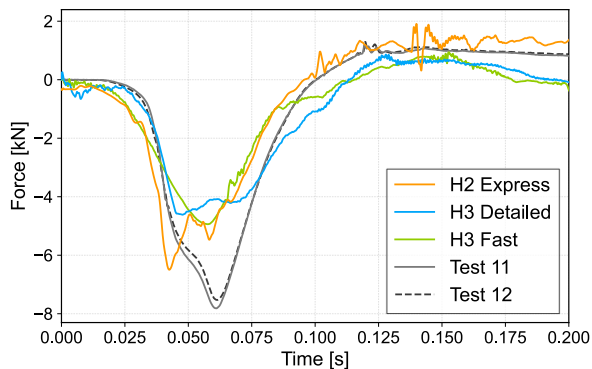
Fig.8:   Scenario 2: lumbar load

Channel	Max error	H2 EXPRESS		H3 DETAILED		H3 FAST	
		Test 11	Test 12	Test 11	Test 12	Test 11	Test 12
Lumbar Fz [%]	15	22.63	20.31	29.28	26.97	33.92	31.79

Table 6: Scenario 2: curve shape error

Channel	Max error	H2 EXPRESS		H3 DETAILED		H3 FAST	
		Test 11	Test 12	Test 11	Test 12	Test 11	Test 12
Lumbar Fz [%]	10	16.88	13.71	40.96	38.71	36.78	34.38

Table 7: Scenario 2: peak error

4.3   Airplane Section: Vertical Impact on Rigid Surface

Table 8 shows the kinematic behavior of the three v-ATDs in the airplane section. For clarity none of the other ATDs present in the simulation are shown. For reference the overall kinematic behavior of the airplane section with only H3 FAST v-ATDs is presented in the second column.
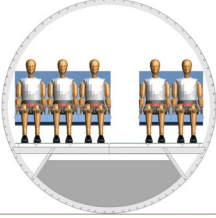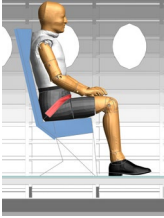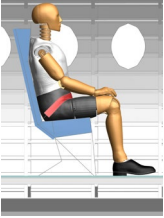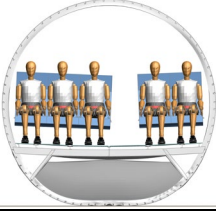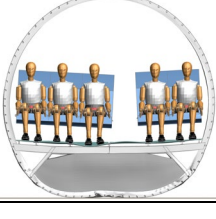
Time	Front View	H2 EXPRESS	H3 DETAILED	H3 FAST
0 s				
0.02 s				
0.04 s				
0.06 s				
0.08 s				
0.1 s				
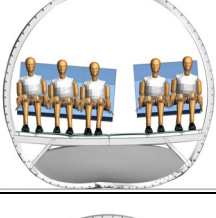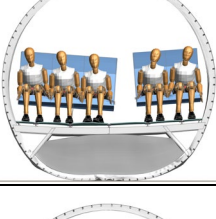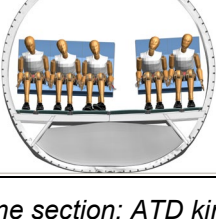
Table 8: Airplane section: ATD kinematics

As seen in the rigid seat tests, the H2 EXPRESS shows a much stiffer behavior in horizontal direction. With the vertical pulse in the airplane section almost no horizontal forward movement is present. Towards the end of the simulation the head of the H2 EXPRESS is even moving backwards. This effect can also be seen in Fig.9 a) for the head CG X-position relative to the seat base. In contrast the H3 FAST v-ATDs upper body bends significantly more forwards. The H3 DETAILEDs upper body does lean forward as well, however not as pronounced as the H3 FAST. This upper body movement affects the

head CG position as shown in Fig. 9 a). There is also a significant difference in initial position which is much larger for the seat with a cushion than the rigid seat.

In the lumbar loads for the vertical crash condition the differences between the v-ATDs become very apparent (Fig. 9 b). Especially the H3 FAST shows a very different lumbar load response to the other two v-ATDs. The maximum compression of -5 kN is considerably lower and the v-ATD exhibits a maximum lumbar flexion of 15 kN, which cannot be observed for the other v-ATDs. In addition, there are comparatively high oscillations in the lumbar load starting at 0.025 s. The difference in lumbar load for the H3 FAST compared to the others is much higher in this case than it is for the 60° rigid seat test. Part of the reason for the deviation of the H3 FAST could be issues with the contact between v-ATD and seat cushion due to the very coarse mesh of v-ATD and seat, leading to penetrations not present in the other two models. Other influences could be the difference in initial position and kinematic behavior. The H2 EXPRESS and the H3 DETAILED exhibit similar maximum lumbar compressive loads, however the curve shapes are different. The H2 EXPRESS experiences the maximum lumbar compression at 0.04 s, whereas the H3 DETAILED shows two extrema of similar severity, both considerably later than the H2 EXPRESS.
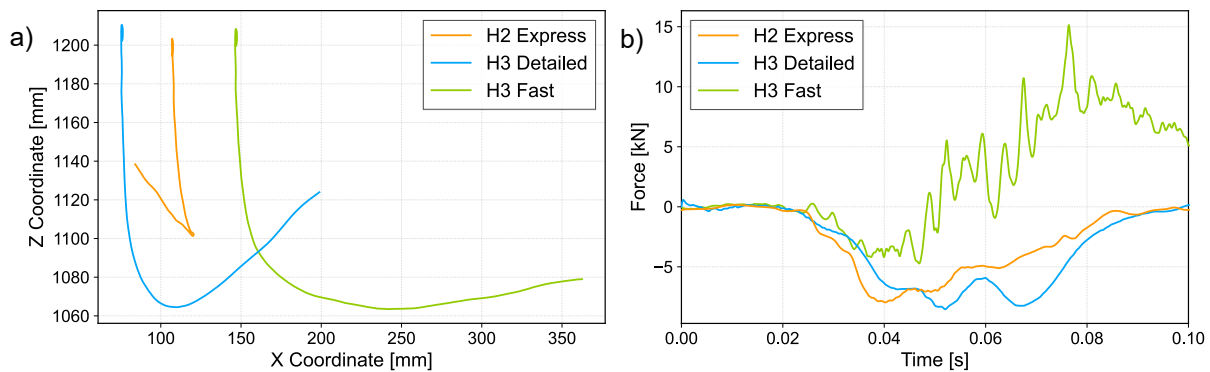

Fig.9:   Airplane section: XZ-position head CG (a) and lumbar load (b)

Fig. 10 shows the vertical acceleration measured at the aisle-side seat/floor interfaces located directly below the v-ATD of interest. For front and rear position an initial negative peak of -30 g and - 24 g respectively can be observed for the three simulations, which can be attributed to the fuselage crash kinematics respectively the cabin floor dynamic response. Subsequently the models exhibit two peaks of 36 g and 54 g for the front position and 30 g and 44 g for the rear position.
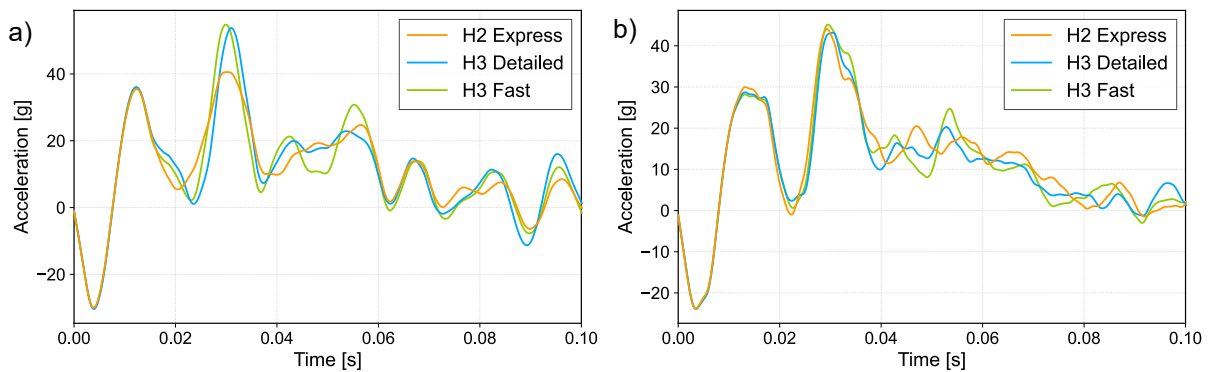

Fig.10: Airplane section: vertical acceleration at the seat track front (a) and rear (b)

The general magnitudes and curve shapes are in good agreement for all three models, except for the second peak at the front location. The model with the H2 EXPRESS shows a 14 g lower peak. Comparing the crash pulses of Fig. 10 with the sled test pulses of Fig. 3 the differences in pulse shape, pulse amplitude and pulse duration are obvious. It confirms the selected approach for the v-ATD evaluation, to consider a real crash scenario in addition to the sled tests to expand the v-ATD evaluation towards more severe crash conditions than represented by the certification specifications.

5   Conclusion and Summary

The preliminary results shown in this paper are the first step in the evaluation of different v-ATD models for aerospace applications. The rigid seat test data supplied by NIAR as supplement to SAE ARP 5765B is a valuable basis for the comparison of different v-ATDs and the validation of modelling approaches. In addition to the validation of aerospace v-ATDs, the data is well suited to evaluate the errors introduced by using e.g. automotive ATDs for aerospace relevant crash scenarios. The additional consideration of a generic airplane section drop test proved to be useful in assessing the transferability of trends seen in sled tests to typical aerospace crash scenarios. Therefore, the presented systematic approach is confirmed to be reasonable as a means to compare various v-ATDs under aerospace crash loading. During the continued phase one of the research plan at DLR, the investigation of the effects of initial v-ATD position will be extended. The evaluation of the three v-ATDs will be expanded by scenario 3 and scenario 4 of the test data. Further steps will include applying the evaluation, using the rigid seat and airplane section, to additional v-ATDs and HBMs.

6   Literature

[1] European Union Aviation Safety Agency: "Certification Specifications and Acceptable Means of Compliance for Normal, Utility, Aerobatic, and Commuter Category Aeroplanes", EASA CS-23 Amendment 4, 2015
[2] European Union Aviation Safety Agency: "Certification Specifications and Acceptable Means of Compliance for Large Aeroplanes", EASA CS-25 Amendment 27, 2021
[3] European Union Aviation Safety Agency: "Certification Specifications, Acceptable Means of Compliance and Guidance Material for Small Rotorcraft", EASA CS-27 Amendment 10, 2023
[4] European Union Aviation Safety Agency: "Certification Specifications, Acceptable Means of Compliance and Guidance Material for Large Rotorcraft", EASA CS-29 Amendment 11, 2023
[5] Federal Aviation Administration: "Airworthiness Standards: Normal, Utility, Acrobatic, and Commuter Category Airplanes", Title 14 CFR Part 23, 2016
[6] Federal Aviation Administration: "Airworthiness Standards: Transport Category Airplanes", Title 14 CFR Part 25, 2023
[7] Federal Aviation Administration: "Airworthiness Standards: Normal Category Rotorcraft", Title 14 CFR Part 27, 2023
[8] Federal Aviation Administration: "Airworthiness Standards: Transport Category Rotorcraft", Title 14 CFR Part 29, 2023
[9] Federal Aviation Administration: "Dynamic Evaluation of Seat Restraint Systems and Occupant Protection on Transport Airplanes", FAA AC 25.562 1B Change 1, 2006
[10] European Union Aviation Safety Agency: "Certification Specifications for Normal-Category Aeroplanes", EASA CS-23 Amendment 5, 2017
[11] Littell, J. D., Putnam, J. B.: "A Summary of ATD Results from a Full-Scale F28 Crash Test", NASA/TM-20210017474, 2021
[12] Sauer, C.: "Entwicklung einer Simulationsmethode für die Gurtmodellierung zur Untersuchung der Insassensicherheit in der Luftfahrt", DLR-IB-BT-ST-2023-94, 2023
[13] Petsch, M., Kohlgrüber, D., Heubischl, J.: " PANDORA - A python based framework for modelling and structural sizing of transport aircraft", MATEC Web of Conferences, Volume 233, 2018
[14] Society of Automotive Engineers: "Analytical Methods for Aircraft Seat Design and Evaluation", SAE Aerospace Recommended Practice 5765B, 2021